A spin-polarized bi-exciton in a semiconductor quantum dot

2008 J. Phys.: Condens. Matter 20 454213

(http://iopscience.iop.org/0953-8984/20/45/454213)

IOP PUBLISHING JOURNAL OF PHYSICS: CONDENSED MATTER

J. Phys.: Condens. Matter **20** (2008) 454213 (5pp) doi:10.1088/0953-8984/20/45/454213

A spin-polarized bi-exciton in a semiconductor quantum dot

Marek Korkusinski[1], Pawel Hawrylak[1] and Marek Potemski[2]

[1] Quantum Theory Group, Institute for Microstructural Sciences, National Research Council, Ottawa, K1A 0R6, Canada

[2] Grenoble High Magnetic Field Laboratory, Centre National de la Recherche Scientifique, Grenoble, France

Received 6 May 2008, in final form 23 June 2008
Published 23 October 2008
Online at stacks.iop.org/JPhysCM/20/454213

Abstract

We discuss the role of spin-polarized multi-exciton complexes in the emission spectra of semiconductor quantum dots. The spin-polarized bi-exciton complex composed of two spin-polarized electrons and two spin-polarized holes confined in a single, parabolic, self-assembled quantum dot is discussed in detail. The configuration-interaction approach is used to compute the energies, wavefunctions, and emission spectra as a function of the magnetic field. It is shown that the spin-polarized bi-exciton emission spectrum differs from the unpolarized spectrum due to the Pauli blocking and exchange interactions. The emission from spin-polarized bi-exciton allows for the measurement of ground and excited single-exciton states, and its magnetic field dependence allows for the differentiation of the spin-polarized bi-exciton and tri-exciton spectrum.

(Some figures in this article are in colour only in the electronic version)

There is currently interest in controlling spin properties at the nanoscale. This can be accomplished by confining spins of carriers to semiconductor quantum dots [1]. The development of, and advances in our understanding of electronic and optical properties of self-organized quantum dots were reported early on at the Winter Schools on Advances in Solid State Physics co-organized in Mauterndorf, Austria, by Professor Günther Bauer [2]. Here we report on the recent progress in theoretically identifying and understanding the spin-polarized electron–hole complexes in semiconductor quantum dots. Such complexes can be generated by resonant circularly polarized excitation, injection from spin-polarized leads [3], during relaxation of carriers after nonresonant excitation, and produced as final states in the radiative recombination. The generation of a spin triplet bi-exciton ($XXTT_1$), spin singlet bi-exciton ($XXSS_1$) and an excited state of the spin singlet bi-exciton ($XXSS_2$) as final states of the emission from the three-exciton (XXX) complex are shown in figure 1(a).

For nonresonant excitation, the emission spectra of even a single quantum dot represent the average over many temporal quantum dot states, with a varying number of excitons and fluctuating charge. This averaging makes it difficult to unambiguously relate measured and theoretically predicted spectra. Recent advances in photon-correlation spectroscopy [4] will allow to 'undress' the measured spectra and compare them with theory. Here we focus on a theory of spin-polarized bi-exciton complex, and relate its properties to the single- and triple-exciton complex. There are several reasons why spin-polarized bi-exciton complex is of interest. Firstly, due to the exclusion principle the spin-polarized bi-excitons ($XXTT$) can only exist when excitons are confined to a quantum dot. Secondly, the spin-polarized carriers occupy two different electronic shells and hence provide means of probing s and p shells at low excitation powers. Thirdly, the emission from $XXTT$ leaves exciton in ground and excited states and provides a tool for measuring the single-exciton spectrum without the need to do difficult absorption measurements. Preliminary theory of a spin-polarized bi-exciton as a final state in the emission from the three-exciton complex has been developed [5] and spin-polarized bi-excitons observed experimentally [6]. Here we present a theory of $XXTT$ as an initial state in the emission process. We identify the spectral features in the emission spectra resulting from the spin polarization of carriers. The spectra of X, $XXSS$, $XXTT$ and XXX as a function of the magnetic field are calculated and the features allowing for the identification of these complexes elucidated.

We model the confinement potential of a single self-assembled dot (SAD) by that of a two-dimensional harmonic

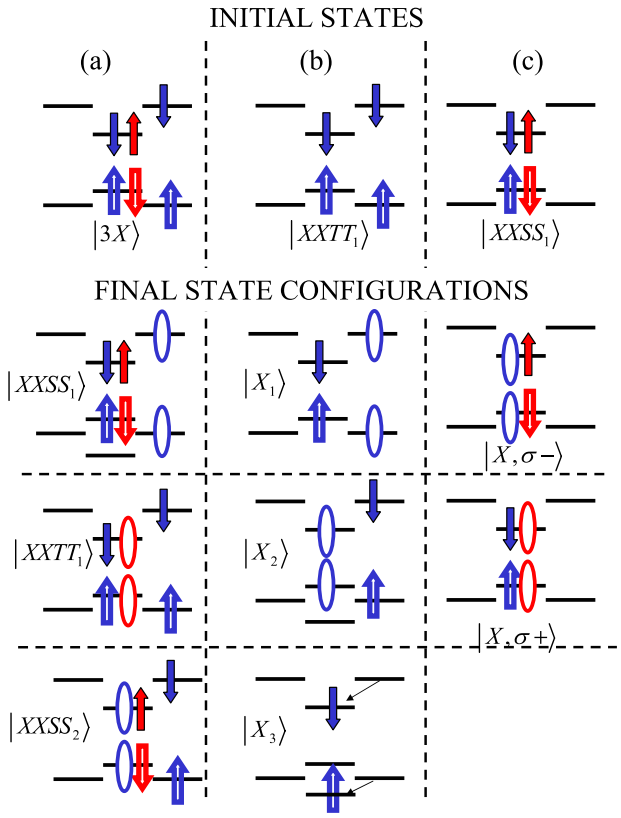

Figure 1. Configurations of the three-exciton complex (a), triplet bi-exciton (b), and the singlet bi-exciton (c). Upper diagrams show the initial-state configurations, and the lower diagrams—the final-state configurations in the emission process.

oscillator (HO) with confinement energy Ω_0^α, where α = e(h) for electrons (holes). The corresponding single-particle energy levels are denoted as $|n_\alpha, m_\alpha, \sigma_\alpha\rangle$, where $n, m = 0, 1, \ldots$ are the HO quantum numbers, and $\sigma = \downarrow, \uparrow$ denotes the z component of the single-particle spin. Due to the cylindrical symmetry of the system the single-particle states are characterized by the angular momentum $l^{\rm e} = n_{\rm e} - m_{\rm e}$ and $l^{\rm h} = m_{\rm h} - n_{\rm h}$ (opposite sign of $l^{\rm h}$ is due to the opposite charge of the hole). In the presence of an external magnetic field $\vec{B} = [0, 0, B]$ perpendicular to the SAD plane, the energies corresponding to the HO orbitals are $E^\alpha(n_\alpha m_\alpha \sigma_\alpha) = \Omega_+^\alpha(n_\alpha + 1/2) + \Omega_-^\alpha(m_\alpha + 1/2)$, where $\Omega_\pm^\alpha = \Omega_{\rm h}^\alpha \pm \Omega_{\rm c}^\alpha/2$, the hybrid energy $\Omega_{\rm h}^\alpha = \sqrt{(\Omega_0^\alpha)^2 + (\Omega_{\rm c}^\alpha)^2/4}$, and the cyclotron energy $\Omega_{\rm c}^\alpha = |e|B/m_\alpha^* c$. Further, $|e|$ and m_α^* are the carrier charge and effective mass, respectively, and c is the speed of light. Note that in our analysis we neglect the Zeeman effect. At zero magnetic field the single-particle states are arranged into shells with increasing degeneracy (one state s, two p, three d etc), while at very large magnetic fields the states with the same quantum number n form quasi-degenerate Landau levels, separated by the cyclotron gap $\Omega_{\rm c}^\alpha$. In the following we express all energies in terms of electronic effective Rydberg, $\mathcal{R} = m_{\rm e}^* e^4/2\varepsilon^2\hbar^2$, and lengths in terms of effective Bohr radius, $a_{\rm B} = \varepsilon\hbar^2/m_{\rm e}^* e^2$, where ε is the dielectric constant of the material. With $m_{\rm e}^* = 0.054 m_0$ and $\varepsilon = 12.4$ we have $\mathcal{R} = 4.78$ meV and $a_{\rm B} = 12.2$ nm. In our model calculation we consider the SAD confinement with $\Omega_0^{\rm e} = 10$ meV $= 2.092\mathcal{R}$ and $\Omega_0^{\rm h} = 5$ meV $= 1.046\mathcal{R}$, compatible with InAs/InP quantum dots.

If we denote the creation (annihilation) operator of an electron on the HO state $|i\rangle \equiv |nm\sigma\rangle$ by $c_i^\dagger$ (c_i), and the analogous operators of the hole by $h_i^\dagger$ (h_i), we can write the Hamiltonian of N interacting electron–hole pairs as

$$\hat{H} = \sum_i E^{\rm e}(i) c_i^\dagger c_i + \sum_i E^{\rm h}(i) h_i^\dagger h_i + \tfrac{1}{2}\sum_{ijkl}\langle ij|V_{\rm ee}|kl\rangle c_i^\dagger c_j^\dagger c_k c_l + \tfrac{1}{2}\sum_{ijkl}\langle ij|V_{\rm hh}|kl\rangle h_i^\dagger h_j^\dagger h_k h_l - \sum_{ijkl}\langle ij|V_{\rm eh}|kl\rangle c_i^\dagger h_j^\dagger h_k c_l. \quad (1)$$

In the above Hamiltonian, the first and second terms account for the single-particle energies, while the remaining terms describe the electron–electron (e–e), hole–hole (h–h), and electron–hole (e–h) interactions. The interaction terms include Coulomb matrix elements $\langle ij|V_{\alpha\beta}|kl\rangle$, which for the HO confinement are computed analytically [7]. If the electrons and the holes are confined by an identical effective SAD potential, i.e., when $m_{\rm e}^*\Omega_0^{\rm e} = m_{\rm h}^*\Omega_0^{\rm h}$, the e–e, h–h, and e–h elements involving the same HO orbitals are equal, and can be expressed in units of $V_0 = \langle 0, 0|V_{\rm ee}|0, 0\rangle = \sqrt{\pi\Omega_{\rm h}^{\rm e}}$ [7].

We expand the many-body eigenstates of the Hamiltonian (1) in terms of the electron–hole configurations. We create all possible configurations of N electron–hole pairs on the single-particle orbitals, form the Hamiltonian matrix in the basis of these configurations, and diagonalize this matrix numerically to obtain eigenenergies. For a given N the number of possible configurations is set by the number of electron and hole single-particle states $M = M_{\rm e} + M_{\rm h}$ selected for the calculation, and depends factorially both on N and M. To reduce the basis size, we label the configurations by the total angular momentum L and total projections of carrier spin $S_z^{\rm e}$ and $S_z^{\rm h}$. Since the Hamiltonian commutes with each of the three operators, we carry out exact diagonalizations in each of these subspaces separately.

Having obtained the eigenenergies and eigenfunctions of the systems of N and $N-1$ electron–hole pairs, we proceed to calculating the emission spectra from Fermi's Golden Rule

$$I(\omega) = \sum_f |\langle f, N-1|\hat{P}^-|i, N\rangle|^2 \delta(E_i - E_f - \omega), \quad (2)$$

where $|i, N\rangle$ and $|f, N-1\rangle$ are the initial and final states in the recombination process, respectively, E_i, E_f are the corresponding energies, and $\hat{P}^- = \sum_{i\sigma} c_{i,\sigma} h_{i,-\sigma}$ is the interband polarization operator. We can divide this operator into two terms: one, $\hat{P}_{\sigma+}^- = \sum_i c_{i,\downarrow} h_{i,\uparrow}$, removes the electron–hole pair in which the electron is spin-down, and the hole-spin-up, leading to the emission of $\sigma+$ polarized photon. The second component, with the opposite alignment of spins, is responsible for the emission of $\sigma-$ polarized photon.

We now turn to the analysis of spin in the multi-exciton complexes ($N = 1 - 3$), following our earlier work in [5].

The dominant single-exciton configuration X_1, shown in figure 1(b), involves an electron–hole pair occupying the

lowest-energy single-particle states. The energy of such an exciton is $E_X = E^{\mathrm{e}}(00\downarrow) + E^{\mathrm{h}}(00\uparrow) - V_0 - \Delta E_X^{\mathrm{corr}}$, where the first two terms account for the single-particle energies of the two carriers, the third term is the Coulomb attraction between them, and the last term represents a correlation energy arising from mixing with higher-energy configurations by Coulomb interactions. Since the final state in the recombination of a single exciton is the vacuum, the above energy will also define the position of the excitonic emission peak. The lowest-energy configuration of the unpolarized bi-exciton, $XXSS_1$, is shown in figure 1(c). It is composed of two electron–hole pairs occupying the s-shell orbitals. The energy of this singlet–singlet configuration, $E_{XXSS} = 2E_{\mathrm{s}} - \Delta E_{XXS}^{\mathrm{corr}}$, with $E_{\mathrm{s}} = E^{\mathrm{e}}(00\downarrow) + E^{\mathrm{h}}(00\uparrow) - V_0$, is composed of two single-exciton energies and the bi-exciton correlation energy. Note that here the two constituent excitons do not interact with one another, as the Coulomb attractive and repulsive terms cancel out. The recombination of one of the two electron–hole pairs leaves the dot occupied with a single exciton X_1, as shown schematically in figure 1(c). Therefore the position of the bi-exciton emission peak is $\omega_{XX} = E_{XXS} - E_X = E_{\mathrm{s}} - (\Delta E_{XXS}^{\mathrm{corr}} - \Delta E_X^{\mathrm{corr}})$. Typically the last term, describing the difference between bi-exciton and exciton correlation energies, is positive. As a result, the bi-exciton emission peak appears at an energy slightly lower than that corresponding to the single exciton. Also, since the recombination of either electron–hole pair is equally probable, the outgoing photons will, on average, be unpolarized. In both the exciton and the singlet–singlet bi-exciton $XXSS$ the carriers occupy predominantly the s-shell levels.

In the triplet–triplet bi-exciton ($XXTT$), on the other hand, we must place the spin-polarized carriers on two different orbitals, belonging to the s and p shell, as shown in figure 1(b). The energy of the electron–hole pair on the p-shell orbital is $E_{\mathrm{p}} = E^{\mathrm{e}}(01\downarrow) + E^{\mathrm{h}}(01\uparrow) - 0.6875V_0$. The energy of the zero-angular momentum configuration $|XXTT_1\rangle$ is $E_{XXTT1} = E_{\mathrm{s}} + E_{\mathrm{p}} - 2V_{\mathrm{sp}}^{XCHG}$, and consists of the energies of the two excitons, the s-shell and the p-shell one, lowered by the e–e and h–h exchange terms $V_{\mathrm{sp}}^{XCHG} = 0.25V_0$. However, there exists a second zero-angular momentum configuration, $|XXTT_2\rangle$ (not shown), with the p-shell exciton occupying the other pair of p-shell orbitals. At zero magnetic field the energy of this configuration is equal to E_{XXTT1}, so these two resonant configurations are strongly mixed by the electron–hole interactions. The resulting $XXTT$ ground state is $|XXTT\rangle = (|XXTT_1\rangle + |XXTT_2\rangle)/\sqrt{2}$, with energy $E_{XXTT} = E_{XXTT1} - 0.1875V_0$. For finite magnetic fields the analysis is more complicated by the fact that the energies E_{XXTT1} and E_{XXTT2} are not equal. Indeed, the configuration $|XXTT_1\rangle$ involves orbitals from the lowest Landau level only, while the high-energy electron–hole pair in the configuration $|XXTT_2\rangle$ occupies the orbitals of the second Landau level. As a result, at low magnetic field there is no linear dependence on the field, while at high magnetic fields the $XXTT$ state is well approximated by the configuration $|XXTT_1\rangle$.

The final states in the process of radiative recombination of the bi-exciton complex are the ground and excited states of a single electron–hole pair with zero total angular momentum [8]. Three examples of the final-state configurations $|X_1\rangle$, $|X_2\rangle$, $|X_3\rangle$ relevant at zero magnetic field are shown schematically in figure 1(b). The energy of the first configuration is simply $E_{X1} = E_{\mathrm{s}}$. The second configuration, $|X_2\rangle$, is an excited state of an exciton in the p shell, and at zero magnetic field it is resonant with a similar p-shell configuration $|X_4\rangle$ (not shown), in which the exciton is placed on the other pair of p-shell orbitals. The two configurations can be mixed in two ways: $|X_2+\rangle = (|X_2\rangle + |X_4\rangle)/\sqrt{2}$, with energy $E_{X2+} = E_{\mathrm{p}} - 0.1875V_0$, and $|X_2-\rangle = (|X_2\rangle - |X_4\rangle)/\sqrt{2}$, with energy $E_{X2-} = E_{\mathrm{p}} + 0.1875V_0$.

The p-shell exciton configuration is also very close in energy with a third configuration $|X_3\rangle$ created by scattering of the electron from the p shell down to the s shell, and simultaneously scattering the hole up to the zero-angular momentum d-shell orbital. In the same way the electron can be scattered up to the d shell and the hole down to the s shell, generating another configuration. These Auger-like configurations have zero- angular momentum, are energetically close to the p-shell exciton, and are mixed by Coulomb interactions. This leads to the splitting of the p-shell exciton, as discussed in [8].

To establish which final-state configurations are optically active, we act on the initial state of the $XXTT$ with the operator $\hat{P}^-_{\sigma+}$. The resulting configuration has nonzero overlap only with the final-state configurations $|X_1\rangle$ and $|X_2+\rangle$. The corresponding emission peak positions are $\omega_{X1} = E_{\mathrm{p}} - 0.6875V_0$ and $\omega_{X2+} = E_{\mathrm{s}} - 0.5V_0$, respectively. These peak positions correspond to the energy of the p-shell and the s-shell electron–hole pair, respectively, but are renormalized by the e–e and h–h exchange terms present in the initial-state energy. In particular, the second peak is expected at energies significantly lower than those of the exciton and singlet bi-exciton emission maxima, and should actually split into two features. The two strong features are visible in figure 2(a), showing the emission spectra of $XXTT$ as high- and low-energy blue bars. Note that with the choice of the alignment of spins, as in the top panel of figure 1(b), it is possible to generate the $\sigma+$ photons only, and therefore the discussed emission spectra are fully polarized.

The splitting of the s-shell recombination into the linear combinations of the $|X_2\rangle$ and $|X_3\rangle$ states results in a small emission maximum appearing at the energy $\omega_{X_3} = E_{\mathrm{p}} - (E^{\mathrm{h}}(11\downarrow) - E^{\mathrm{h}}(00\uparrow) + V_0)$. This energy corresponds to that of the p-shell exciton, lowered by two terms: (i) the difference of single-particle energies of the d and s shells of the hole, and (ii) the Coulomb interaction term V_0. This renormalization is much larger than the exchange terms contributing to the peak position ω_1. As a result, the additional, weak emission maximum is seen in figure 2(a) in the vicinity of the exciton and singlet bi-exciton maxima. The photon emitted at this energy is also $\sigma+$ polarized.

Let us now analyze the emission spectra of the $XXTT$ complex as a function of the magnetic field, shown in figure 3(a). As already mentioned, for sufficiently high fields we can approximate the initial state of the $XXTT$ complex with the configuration $|XXTT_1\rangle$. The final states, on the other hand, are well represented by the configurations $|X_1\rangle$, $|X_2\rangle$, and $|X_3\rangle$. Out of these three states, the first and the

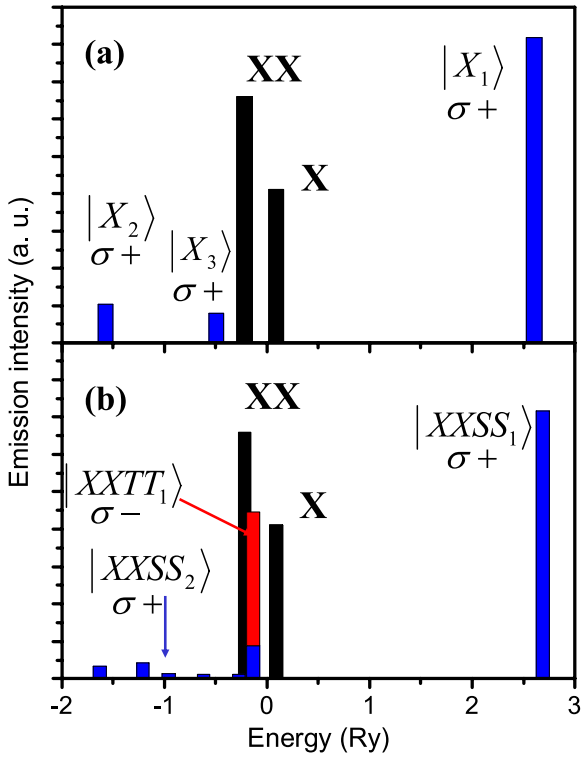

Figure 2. Emission spectra of the triplet bi-exciton (a) and the three-exciton system (b) at zero magnetic field. Black bars correspond to the exciton (X) and singlet bi-exciton (XX) emission peaks. Labels of the maxima of triplet bi-exciton and the three-exciton complex identify the final states shown in figure 1(b) and (c), respectively. Blue (red) color denotes $\sigma+$ ($\sigma-$) polarization of outgoing photons.

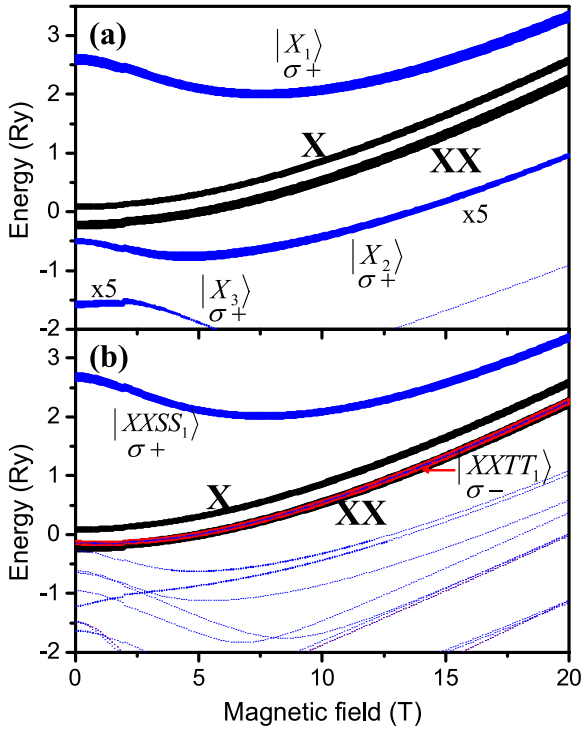

Figure 3. Emission spectra of the triplet bi-exciton (a) and the three-exciton system (b) as a function of the magnetic field. Labels and color coding match those in figure 2.

second are built out of lowest Landau level orbitals only, while in the optically forbidden configuration $|X_3\rangle$ the hole is placed on the second Landau level orbital. The energy $E_1 = \Omega_h^e + \Omega_h^h - V_0$ exhibits a diamagnetic shift towards higher energies with the increase of the magnetic field, while the energy $E_2 = \Omega_h^e + \Omega_-^e + \Omega_h^h + \Omega_-^h - 0.6875V_0$ decreases as the field grows. On the other hand, for small fields the energy $E_3 = \Omega_h^e + 2\Omega_h^h - 0.6875V_0$ is smaller than E_2, but larger than E_1. As the field grows, however, this energy increases, and becomes larger than E_2. Since the optically forbidden state $|X_3\rangle$ is separated from the optically active configurations $|X_1\rangle$ and $|X_2\rangle$ by an increasing energy gap, the Coulomb mixing of these configurations becomes less effective, and the emission amplitude of the corresponding emission peak decreases. This is exactly the behavior observed in figure 3(a). At zero magnetic field we start with the familiar three-peak structure of the emission spectrum, with the low-amplitude middle maximum in the vicinity of the exciton and bi-exciton features. As we increase the magnetic field, the high-energy peak, corresponding to the emission of the p-shell exciton, shifts first to lower, and then to higher energies. For small fields, the lowest-energy peak, corresponding to the emission of the s-shell exciton, blue-shifts, following the analogous behavior of the exciton and singlet bi-exciton maxima. At the same time the small, forbidden maximum undergoes a rapid shift towards smaller energies. Further, the two low-energy maxima anticross. The middle maximum takes on the character of the usual s-shell emission, and its evolution mirrors that of the exciton and unpolarized bi-exciton lines (marked in black). Note, however, that the $XXTT$ is separated from these two by an exchange gap, which widens as the field grows. On the other hand, the lowest-energy maximum takes on the character of the forbidden transition, rapidly red-shifts and becomes dark.

Let us now compare the emission spectra of the $XXTT$ with those of a three-exciton complex XXX. The optical properties of the SAD confining three electron–hole pairs have been discussed in detail in [5]. One of the two lowest-energy configurations of the complex at zero magnetic field, $|3X\rangle$, is shown schematically in figure 1(a) (first diagram from the top), while the other one (not shown) is created by placing the p-shell electron–hole pair on the other pair of p-shell orbitals. Thus, the ground state of the system differs from that of the $XXTT$ only by the presence of the additional s-shell exciton, marked in figure 1(a) in red. In analogy to $XXTT$, the zero-field ground state of the system is a linear combination of the two configurations, while at high magnetic fields the ground state is well approximated by $|3X\rangle$. The most important final states in the radiative recombination of the triple exciton are shown in figure 1(a) (second, third, and fourth diagram from the top). The lowest-energy final state, $|XXSS_1\rangle$, is composed of the two electron–hole pairs placed on the s shell. The energy of the photon radiated in this process falls in the range of the p-shell emission and is nearly identical to that of the p-shell maximum of $XXTT$, as shown in figure 2(b) for zero magnetic field. Indeed, the only difference between these two systems is the presence of the additional s-shell

electron–hole pair (marked in red), which does not interact with the other two pairs, and therefore has no influence on the p-shell emission process. The fundamental difference between the two- and three-exciton systems is visible in the emission from the s shell, involving the remaining two final states from figure 1(a), i.e., $|XXTT_1\rangle$ and $|XXSS_2\rangle$. The final state $|XXTT_1\rangle$ is obtained by removing the red electron–hole pair from the s shell in the state $|3X\rangle$, thus leaving two spin-polarized electrons and two spin-polarized holes i.e., the triplet bi-exciton $XXTT$. The outgoing photon carries no exchange interaction energy, and therefore the corresponding emission maximum should coincide with that of a single exciton, with possible small deviations due only to correlation effects, as shown in figure 2(b). Note that the polarization of this photon is opposite to that obtained from the p shell. As for the final state $|XXSS_2\rangle$, its total spin is not determined. We must create the correct final states by creating linear combinations of all configurations with the same orbital occupation as $|XXSS_3\rangle$ and the same total spin projections of electrons and holes (in one of such configurations the hole configuration is unchanged, but the electron spins are interchanged). Altogether we can create four such states: an electron triplet–hole triplet configuration, a singlet–singlet one, and two mixed-spin states: singlet–triplet and triplet–singlet. Out of these four the first one has the lowest energy due to the e–e and h–h exchange, and therefore will contribute to the highest-energy emission peak. This peak will coincide with the one corresponding to the final state $|XXTT_1\rangle$, but will have the opposite polarization. The remaining emission maxima, in order of decreasing energy, are those corresponding to the mixed-spin and the singlet–singlet configurations. It is also possible to generate optically forbidden configurations similar to $|X_3\rangle$ discussed in the case of the $XXTT$ complex. One of such configurations is created by removing one hole from the s shell of configuration $|XXSS_1\rangle$ and replacing it on the d-shell orbital. The position of the emission peak corresponding to such a final state depends upon the details of the confinement and interaction energies. In our case this peak is seen just below the peak corresponding to the recombination to the triplet–triplet final state, and is marked in figure 2(b). Note, however, that such a forbidden transition must necessarily be of the electronic singlet character due to the distribution of both electrons on the s shell, while the hole spin can be singlet or triplet. As a result, this configuration does not mix with the triplet–triplet final state. This property is crucial in understanding the magnetic field evolution of the spectra of the three-exciton system, shown in figure 3(b). The p-shell line evolves in exactly the same manner as the analogous line of the $XXTT$ complex. However, the evolution of the strong maximum seen in the s-shell energy region is nearly identical to that of the single exciton. It remains strong throughout the entire region of magnetic fields and does not exhibit any anticrossings in spite of the presence of additional emission maxima (allowed and forbidden) at similar energies.

In summary, we have analyzed the role of spin in the emission spectra of the spin-polarized bi-exciton $XXTT$ complex as a function of the magnetic field. The $XXTT$ is found to emit in the s shell just like the spin-unpolarized bi-exciton $XXSS$ as well as in the p-shell spectral range just like the three-exciton complex. These features of the spin-polarized $XXTT$ allow us to probe the exciton ground and excited states. These final excited states involve a number of configurations with a characteristic dependence on the magnetic field which allows to distinguish the emission from the $XXTT$ complex from the emission from the three-exciton complex. The emission energy of $XXTT$ is shown to be red-shifted from the exciton and unpolarized bi-exciton energy by the s–p shell exchange interaction. It is hoped that these predictions will help in identifying spin-polarized bi-excitons in the emission spectra of semiconductor quantum dots.

Acknowledgment

The authors thank the NRC-CNRS Collaborative Research Grant for support.

References

[1] Michler P (ed) 2003 *Single Quantum Dots: Fundamentals, Applications, and New Concepts* (*Topics in Applied Physics* vol 90) (Berlin: Springer)
[2] Hawrylak P and Wojs A 1996 Electronic structure and optical properties of self-assembled quantum dots *Proc. 9th Winter School on New Developments in Solid State Physics (Mauterndorf, Austria, Feb. 1996)* ed G Bauer, F Kuchar and H Heinrich; *Semicond. Sci. Technol.* **11** 1516
[3] Kioseoglou G, Hanbicki A T, Sullivan J M, van 't Erve O M J, Li C H, Erwin S C, Mallory R, Yasar M, Petrou A and Jonker B T 2004 *Nat. Mater.* **3** 799
[4] Suffczyński J, Trajnerowicz A, Kazimierczuk T, Pi etka B, Kowalik K, Kossacki P, Golnik A, Nawrocki M, Gaj J A, Wysmołek A, St epniewski R, Potemski M and Thierry-Mieg V 2007 *Acta Phys. Pol.* A **112** 461
[5] Hawrylak P 1999 *Phys. Rev.* B **60** 5597
[6] Bayer M, Stern O, Hawrylak P, Fafard S and Forchel A 2000 *Nature* **405** 923
[7] Jacak L, Hawrylak P and Wojs A 1998 *Quantum Dots* (Berlin: Springer)
[8] Narvaez G A and Hawrylak P 2000 *Phys. Rev.* B **61** 13753